



HAL
open science

Rock Fragmentation by High-Voltage Pulses

Marwa Dakik, Hedi Sellami, Ahmed Rouabhi, Isabelle Thenevin, Kathy Bru,
Yannick Ménard

► **To cite this version:**

Marwa Dakik, Hedi Sellami, Ahmed Rouabhi, Isabelle Thenevin, Kathy Bru, et al.. Rock Fragmentation by High-Voltage Pulses. 12th conference of the French Society of Electrostatics, Jul 2023, Cherbourg en Cotentin, France. hal-04128631

HAL Id: hal-04128631

<https://hal.science/hal-04128631>

Submitted on 14 Aug 2023

HAL is a multi-disciplinary open access archive for the deposit and dissemination of scientific research documents, whether they are published or not. The documents may come from teaching and research institutions in France or abroad, or from public or private research centers.

L'archive ouverte pluridisciplinaire **HAL**, est destinée au dépôt et à la diffusion de documents scientifiques de niveau recherche, publiés ou non, émanant des établissements d'enseignement et de recherche français ou étrangers, des laboratoires publics ou privés.

Rock Fragmentation by High-Voltage Pulses

M. DAKIK¹, H. SELLAMI¹, A. ROUABHI¹, I. THENEVIN¹, K. BRU², Y. MENARD²

¹Mines Paris, PSL University, Center for geosciences and geoen지니어ing, 77300 Fontainebleau, France

²BRGM, F-45060 Orléans, France

Abstract— Rock breaking is an essential operation in mining engineering, as well as in the exploitation of natural resources such as geothermal, oil, and gas drilling. High Voltage Pulse Fragmentation (HVPF) has demonstrated the potential for lower specific energy consumption compared to mechanical methods when dealing with hard rocks. An accurate understanding of the physical mechanism behind the HVPF process is necessary to optimize the competitiveness of this technique and promote its industrial-scale deployment. HVPF involves delivering a fast-rising voltage pulse of hundreds of kilovolts to a rod electrode in contact with a specimen, which rests on a grounded electrode plate. This paper presents experimental results for two materials: concrete and sandstone in both dry and saturated states. The specimens were subjected to 90 kV electrical discharges with single and multiple pulses. In dry and saturated sandstone specimens, small craters formed on both sides, while radial tensile cracks propagating from the channel along the aggregate boundaries were observed in concrete. A complete channel passing through the specimens and joining the two electrodes was also observed. Furthermore, the repetition of pulses exponentially increased the volume of the crater, highlighting the cumulative effect of pulse repetition on the rock fragmentation process. These experimental observations suggest that the discharge likely occurs in a direct mode.

Keywords: Electrical discharge, voltage, HVPF, rock fragmentation, concrete, sandstone

I. INTRODUCTION

Rock breaking is an essential operation in mining engineering, geothermal exploration, and oil and gas drilling. As the exploitation of natural resources increases, achieving optimal rock fragmentation becomes increasingly challenging. The commonly employed techniques include traditional mechanical rock breaking, the drilling-blasting method, and the full-face tunnel boring machine (TBM). However, these methods have limitations, including low energy efficiency and high costs [1]. Moreover, the application of drilling-blasting methods is accompanied by stringent safety and environmental constraints, given that blasting generates toxic fumes, ground vibrations, and dust. Given these constraints, there is a growing interest in transitioning away from conventional rock fragmentation methods.

Energy consumption constitutes up to a quarter of the total operational cost in many hard rock mining operations, with as much as half of this energy attributed to rock fragmentation using conventional mechanical crushing and grinding methods [2]. These prevailing methods fragment rocks in a non-selective manner, where all feed particles, including barren particles with no economic value, are crushed and finely ground for further processing. Consequently, a significant amount of energy is wasted on grinding barren material. Therefore, the development of selective fragmentation methods and the implementation of strategies for the early removal of barren material in the comminution flowsheet are imperative [3]. A further advantage of such selective methods is the generation of cracks specifically at grain boundaries, enabling the liberation of valuable components at a coarser size and thereby reducing the need for intensive grinding [4].

As a result, novel crushing and grinding techniques have emerged, including high-voltage electrical pulse methods. The technique of high-voltage pulse fragmentation (HVPF), which has garnered considerable attention, demonstrates remarkable efficiency and substantial developmental potential. Notably, HVPF exhibits the capacity to enhance fragmentation selectivity and reduce energy consumption in rock crushing. Similar energy consumption reductions are observed in drilling applications. For instance, it has been reported that while rotary drilling demands an energy input of 600–950 J/m³, under certain conditions, HVPF technology requires less energy (100–500 J/m³) to break rock [5]. Additionally, HVPF enhances drilling speed in hard rocks compared to the conventional rotary drilling method, and its tools exert minimal mechanical forces on the rock, potentially minimizing tool damage and resulting in smaller, lighter, and safer drilling rigs.

Research on the rock-breaking mechanism through electrical discharge originated at Tomsk University in the 1960s. Based on experiments, Andres (1995) [6] proposed the relationship between the electric breakdown field strength of water (E_0), rock, and oil, and the pulse rising time (τ), as illustrated in Fig. 1. High-voltage pulse methods can be categorized into electro-hydraulic rock breaking and direct electro-pulse rock breaking.

During electric discharge in rock immersed in water, power is released in the form of voltage surges with peaks reaching up to 600 kV. When $\tau > 500$ ns, the breakdown field strength of the rock surpasses that of water, leading to the generation of discharge plasma within the water. This process gives rise to shock waves that propagate toward the rock surface, inducing

fragmentation. This phenomenon, termed electro-hydraulic rock breaking, operates in an indirect or delocalized mode. Conversely, when $\tau < 500$ ns, the breakdown field strength of the rock is lower than that of water. Consequently, the discharge plasma is primarily formed within the rock itself. The expansion of the plasma channel induces stress within the rock, leading to its fragmentation. This mechanism, known as electro-pulse breaking, operates in a direct or localized mode. Research has demonstrated that electro-pulse breaking exhibits higher efficiency in breaking down the same volume of rock compared to electro-hydraulic rock breaking [7].

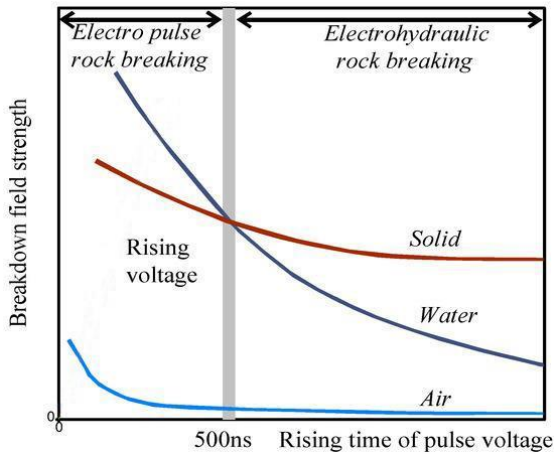


Fig. 1. Schematic representation of the relation between electric breakdown field strength and pulse rising time for solid, water and air [7]

Through experimentation, Cho et al. [8] [9] constructed a curve depicting the variations in current and voltage over time during the breakdown process. They delineated the process of electric fragmentation into three distinct phases: the pre-breakdown phase, the breakdown phase, and the exploding phase, illustrated in Fig. 2.

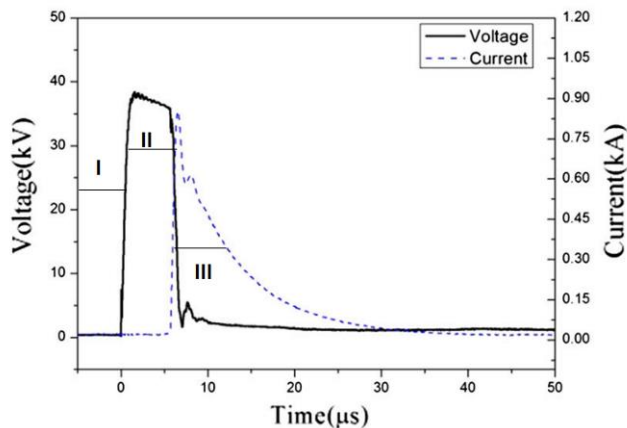


Fig. 2. Three phases of electrical breakdown process [8]

When applying a voltage pulse with $\tau < 500$ ns, the discharge predominantly occurs within the rock. Initially, a plasma channel forms at the tip of the high-voltage electrode, propagating within the rock to connect the

high-voltage electrode and ground electrode, thus establishing a main discharge channel in phase I. The voltage at the high-voltage electrode rapidly decreases, and the current within the channel experiences a swift increase towards the end of phase II. Once the plasma channel is fully formed, the conductivity within the rock experiences a sharp surge, leading to the rapid injection of electric charge into the plasma channel. This, in turn, triggers a rapid rise in temperature within the plasma channel, causing it to expand. Consequently, the rock fractures when the stress exerted by the plasma channel surpasses the rock's inherent strength.

Presently, a comprehensive understanding of the mechanisms underlying mechanical damage caused by electrical discharge in rocks remains elusive. This lack of understanding is reflected in existing models within the literature, which inadequately capture the underlying physics of the process, thereby offering limited guidance for optimizing HVPF parameters. This complexity can be attributed to the multi-physical nature of HVPF, which encompasses a variety of fields, combined with the inherent heterogeneity of processed rocks.

Our overarching objective is to establish an electric breakdown model that encompasses the electric breakdown process under various high-voltage pulses, achieved by coupling the electric, thermal, and mechanical domains. To elucidate the electric breakdown phenomena and their underlying mechanisms, we conducted a series of experimental tests utilizing the SELFRAG machine at BRGM in Orléans, France. This paper details the fracture process of concrete and sandstone during electrical discharge, with voltages reaching up to 90 kV. Specimens with heights (and thus electrode gaps) ranging from 10 to 40 mm were employed. Empirical relationships describing rock damage as a function of electrode gap distance, input voltage, and pulse count were derived. Furthermore, 3D tomography analysis yielded images of the channels within the rock that connect the high-voltage electrode to the ground electrode.

II. ELECTRICAL BREAKDOWN TESTS

A. Tested Specimens

In pursuit of a deeper comprehension of the fundamental principles of HVPF, experimental tests were conducted on Vosges sandstone, a sedimentary rock, and concrete. Table II provides an overview of the physical and mechanical properties of both specimens. Distinguishing characteristics between the specimens include the gap radius between grains, ranging from 10 μm to 100 μm in sandstone and less than 1 μm in concrete. The specimens are cylindrical, with a diameter of 65 mm and varying heights (10, 15, 20, 25, 30, 35, and 40 mm). The composition of concrete, recognized as a heterogeneous material, is displayed in Table I. Sandstone, classified as a medium-hard rock, is considered homogeneous due to

its single-grain composition. Two categories of sandstone were analyzed:

- Saturated sandstone: specimens are soaked in water for more than 24 hours.
- Dry sandstone: specimens are left at room temperature.

Table I
Formulation of concrete materials

w/c = 0.44
White cement quality CEM I 52.5
Water: 14.7% of the total weight
Cement 33.3%
Sand NE 34 42.0%
Gravel 2-4 mm 10.0%

Table II
Physical and mechanical properties

	Sandstone	Concrete
Density (kg/m ³)	2130	2132
Total Porosity %	20%	24.5%
Young's Modulus (MPa)	15600	10948
Uniaxial compressive strength (MPa)	40	53
Uniaxial tensile strength (MPa)	3	3.1
Cohesion (MPa)	13	18

B. HVPF used Setup

The high-voltage pulse machine used in our experiments (Fig. 3) contains three main parts: a high-voltage pulse generator, two electrode systems, and a testing system. The supplied voltage is transformed into a higher voltage, which is transferred to a Marx generator to generate high-voltage pulses. A high-voltage transmission line transmits them into a process vessel containing the specimen submerged in water. The equipment used in our tests is the 'Lab', a laboratory-scale electrostatics high voltage pulse (HVP) batch processing unit manufactured by SELFRAG AG, Switzerland. It has a built-in touch panel where it is possible to set pulse voltage (90 kV - 200 kV), repetition rate/frequency (1 - 5 Hz), electrode gap (10 - 40 mm), and number of pulses (1 - 1000). High-voltage pulses are applied to the electrodes of a few diameters with a pin-to-plate configuration. This experimental device is designed for batch processing of specimens up to approximately 1 kg. The processing vessel is filled with de-ionized water to limit the number of variables inside the system. Our tests were performed with a voltage of 90 kV and a pulse frequency of 5 Hz. The first series of experiments was carried out with the sandstone to investigate the influence of the saturation and the electric field, considering the different specimen heights/electrode gaps. The second series was performed with the concrete to investigate the influence of the electric field considering different specimen heights/electrode gaps.

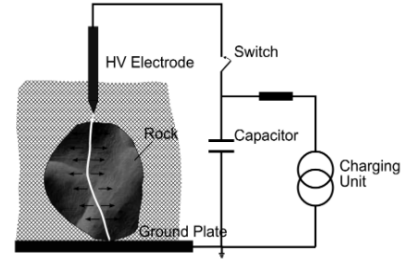


Fig. 3. Schematic diagram of the experimental setup [10]

C. Results analysis techniques

1. Determination of Crater Volumes with Silastene

After the electrical tests on Vosges sandstone and concrete, the formation of a crater is sometimes observed on each side of the specimens. The top and bottom craters are filled with a mixture of 100g of RTV 148A silastene combined with 10 g of RTV 147B to determine the volume of these craters as precisely as possible. The mixture is left to dry on the specimens for around 24 hours. After weighing the extracted filled volume, the crater's volume is determined, knowing the density of the mixture.

2. CT scanning with X-ray tomography

The X-ray microtomographic acquisitions are performed on an ULTRATOM from RX-solutions. An open microfocus X-ray source is used, coupled to a Varian PaxScan 2520DXi detector flat panel with amorphous silicon and a CsI conversion screen; 1874 × 1496-pixel matrix; pixel pitch of 127 μm; 16 bits of dynamic. The entire specimens are scanned with a spatial resolution of 43.9 μm in a tomography mode. Acquisition parameters are set at 100 kV for tube voltage and 430 μA for tube current. A setting of 12.5 frames per second is used with an averaging of 20 frames per projection. Filtration of the beam is performed using a 1 mm Al filter. Two cross-sectional images are obtained; one is in the X-Y direction where we can see the top face of the treated specimen with the X-Y direction because Z is fixed at the dimension of the top face. The other image is in the Y-Z direction where we can see the complete channel inside the specimen.

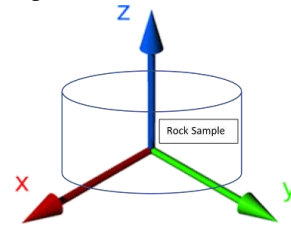


Fig. 4. Geometrical orientation during X-ray tomography

III. RESULTS AND DISCUSSIONS

A. Experimental Results in Sandstone

The top face of the specimen is placed against the high-voltage electrode, and the bottom face against the grounded electrode. Table III shows the macroscopically observed craters on the top and bottom faces of dry sandstone at various values of electric field E (1), and table IV represents the results for saturated sandstone, after treatment with one pulse.

$$E = V/d \quad (1)$$

where V is the maximum delivered voltage, and d is the electrode gap which corresponds to the height of the specimen.

Table III

Electric damage on dry sandstone as function of electric field, after treatment with 1 pulse (voltage fixed at 90 kV)

Electric field	9 kV/ mm	6 kV/mm	4.5 kV/mm	3.6 kV/mm	3 kV/mm	2.57 kV/mm	2.25 kV/mm
Top face 1 pulse							
Bottom face 1 pulse							

Table IV

Electric damage on saturated sandstone as function of electric field, after treatment with 1 pulse (voltage fixed at 90 kV)

Electric field	9 kV/ mm	6 kV/mm	4.5 kV/mm	3.6 kV/mm	3 kV/mm	2.57 kV/mm	2.25 kV/mm
Top face 1 pulse							
Bottom face 1 pulse							

From Tables III and IV, it becomes evident that in nearly all specimens, a single pulse results in the formation of small craters on both sides, indicating a probable occurrence of direct discharge. Macroscopic observation of the tested specimens provides insight into the possibility of evaluating the presence of a channel between the two electrodes and assessing the associated electric field strength. Notably, the experimentation revealed that, in the case of dry sandstone, a minimum field strength of 3.5 kV/mm was necessary for the establishment of a complete channel between the electrodes without inducing substantial specimen fragmentation (in the form of multiple fragments). Conversely, for saturated rock, a field strength as low as 2.57 kV/mm was sufficient to create a complete channel that bridges the two faces of the specimen. Intriguingly, with saturated sandstone, a field of 3.5 kV/mm could fracture the rock into several fragments, reaffirming the notion that dry sandstones possess greater dielectric strength compared to saturated ones.

Figure 5 shows the outcome of a 90 kV discharge on a 20 mm height sandstone, showcasing the phenomenon of channel creation. The presence of a channel traversing the specimen and connecting the two electrodes is evident. Furthermore, it is noteworthy that this discharge

induces three significant fractures without causing complete specimen disintegration.



Fig. 5. Saturated sandstone with a complete channel without fragmentation after HVP treatment

A parallel observation is depicted in Figure 6, illustrating the electrical damage in three dry sandstone specimens at a 15 mm electrode gap, subjected to one, two, and three pulses. In this context, all three specimens exhibit a complete channel connecting the electrodes. However, the specimen subjected to three pulses is found to be totally fragmented. In contrast, the one-pulsed and two-pulsed specimens display major fractures that do not extend to the specimen boundary. These findings imply the influence of cumulative pulse repetition on rock fragmentation, forming the basis for the intricate interplay between electrical discharge and mechanical

failure in rock materials. The cumulative mechanical consequences arising from pulse repetition are discernible in the volume of the crater created within the specimen. These experimental results highlight the crucial role of pulse repetition in shaping the interaction between electrical discharge and mechanical behavior, underscoring its impact on the formation and propagation of fractures in rocks.



Fig. 6. Electric damage of dry sandstone under 1, 2, and 3 pulses, respectively (voltage fixed at 90 kV, electric field = 6 kV/mm)

Indeed, Fig. 7. illustrates the variation of the crater's volume on the top and bottom faces of the specimen, i.e., around each of the two electrodes, as a function of the number of pulses. It shows that the repetition of the pulse increases exponentially the volume of the crater. Moreover, we can deduce that the volume of the upper crater is greater than the bottom one, which is related to the difference in profile between the top electrode and the bottom electrode.

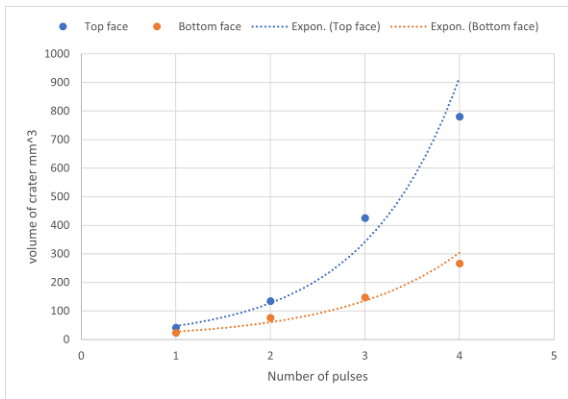


Fig. 7. Volume of crater as function of number of pulses for dry sandstone (voltage fixed at 90 kV, electric field = 4.5 kV/mm)

B. Experimental Results in concrete

Table V shows electrical damage on the top face of concrete as a function of the electric field after treatment with one pulse performed at 90 kV. Experimental results show that specimens treated with an electric field of less than 4.5 kV/mm are unfragmented, meaning that concrete needs more energy to be damaged. Besides, Table V shows the macroscopically observed damage on concrete as a function of the electric field, E. After the specimen's breakdown, more cracks extend in the radial direction, which is consistent with the results obtained in [6]. Moreover, unlike for sandstones, the volume of craters around the electrodes is less obvious. This difference could be explained by a different gap radius

between the grains, even if the sandstones have a lower porosity than the concrete ones (20% vs 24.5%). Indeed, the larger gap radius R between the grains in sandstone ($10 \mu\text{m} < R < 100 \mu\text{m}$ for sandstone vs $R < 1 \mu\text{m}$ for concrete) could lead to fewer fractures extension and more local decohesion (thin hole formation between electrodes), preventing then the formation of radial cracks. These limited radial cracks can explain why the pressure developed in the channel is not enough to create sufficient pressure to fragment the sandstone while breakage is observed for the concrete one for the same electric field. Furthermore, decreasing the electrical field results in less impact on the specimen which is like what has been observed for the sandstone.

Table V

Electrical damage on concrete as function of electric field, after treatment with 1 pulse and voltage = 90 kV

9 kV/mm	6 kV/mm	4.5 kV/mm
 CON_10_1	 CON_15_3	 CON_20_1
3.6 kV/mm	3 kV/mm	2.57 kV/mm
 CON_25_1	 CON_30_2	 CON_35_4

C. CT scanning with X-ray tomography

Two unbroken specimens after HVPF treatment were subjected to CT scanning with X-rays to observe the formation of plasma channels inside the specimen. The contrast in the images shows the differences in the density of the minerals; the white portions indicate high-density minerals, such as sandstone, concrete, and aggregates, while the black parts are volumes filled with air. Fig. 8a. shows the radial tensile cracks propagating from the center along the boundaries of the aggregates in treated concrete, while Fig. 8b shows the resultant fracture pattern of the HVP-treated sandstone, where the top face crater and some radial cracks propagating are shown. These observations reveal that radial cracks are more likely to occur in concrete than in sandstone. As indicated before, this could be explained by a different gap radius between the grains. The gas (water vapor and others) could then leave the sandstone through this porosity producing only a limited number of cracks.

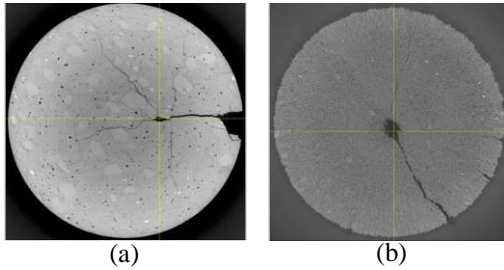


Fig. 8. Selected cross-sectional image X–Y slices of the tested specimens. (a) concrete (b) sandstone

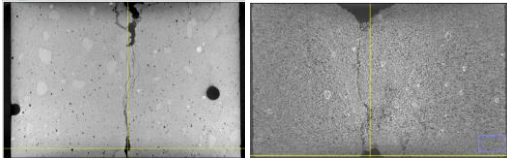


Fig. 9. Selected cross-sectional image Y–Z slices of the tested specimens. (a) concrete (b) sandstone

Fig. 9.a and Fig. 9.b show the propagated channel from the high voltage electrode to the ground electrode inside the specimens. These figures confirm that the formation of the channel penetrating the two ends of electrodes is not always accompanied by the mechanical fragmentation of the rock.

V. CONCLUSIONS

The primary objective of this paper is to contribute to an enhanced comprehension of the physical phenomena inherent in High-Voltage Pulse Fragmentation (HVPF). We have established empirical relationships that link breakdown damage to variables including electrode gap distance, input voltage, and pulse count. Additionally, we have harnessed tomography analysis to obtain clear visual representations of the channels connecting the high-voltage electrode to the ground electrode.

Key insights gleaned from this research can be summarized as follows:

1. **Electric Field Influence:** Within a consistent rock sample and under identical voltage conditions, an increase in electrode gap distance is found to result in diminished rock damage. Evidently, the electric field strength exhibits a significant impact on the extent of rock damage. Furthermore, elevating the pulse count leads to an exponential escalation in the volume of rock craters formed.
2. **Direct Discharge Indication:** Under the conditions examined in this study, it has been consistently observed that a single pulse is adequate to create small craters on both sides of nearly all rock specimens. This trend strongly suggests that discharge predominantly transpires in a direct mode.

3. **Dielectric Strength Comparison:** Dry sandstones exhibit superior dielectric strength compared to their saturated counterparts. Specifically, the minimum electric field strength required to establish a complete channel between electrodes is found to be 36% higher in dry sandstone in comparison to saturated sandstone.
4. **Plasma Channel Formation:** The creation of a plasma channel bridging the electrode ends is not invariably accompanied by mechanical fragmentation of the rock. Nevertheless, it constitutes an indispensable prerequisite for the process of electrical crushing within HVPF.
5. **Cumulative Mechanical Effects:** The repetition of pulses remarkably accentuates the volume of rock craters formed, significantly impacting the fragmentation process. This cumulative mechanical damage within the rock, stemming from pulse succession, is likely fundamental to the intricate interplay between electrical discharge and mechanical failure in rock materials.

In essence, this study contributes important insights into the complex interactions encompassing HVPF, thereby advancing our understanding of this intriguing process.

REFERENCES

- [1] Wang, S., Guo, Y., Cheng, G., & Li, D. (2017). Performance study of hybrid magnetic coupler based on magneto thermal coupled analysis. *Energies*, 10(8), 1148.
- [2] Huang, Wei, and Yumeng Chen. "The application of high voltage pulses in the mineral processing industry-A review." *Powder Technology* 393 (2021): 116-130.
- [3] Wang, Eric, Fengnian Shi, and Emmy Manlapig. "Mineral liberation by high voltage pulses and conventional comminution with same specific energy levels." *Minerals Engineering* 27 (2012): 28-36.
- [4] Bru, Kathy, et al. "Comparative laboratory study of conventional and Electric Pulse Fragmentation (EPF) technologies on the performances of the comminution and concentration steps for the beneficiation of a scheelite skarn ore." *Minerals Engineering* 150 (2020): 106302.
- [5] Biela, J., Marxgut, C., Bortis, D., & Kolar, J. W. (2009). Solid state modulator for plasma channel drilling. *IEEE Transactions on Dielectrics and Electrical Insulation*, 16(4), 1093-1099.
- [6] Andres, U. (1995). Electrical disintegration of rock. *Mineral Processing and Extractive Metallurgy Review*, 14(2), 87-110.
- [7] Li, Changping, et al. "Influences on high-voltage electro pulse boring in granite." *Energies* 11.9 (2018): 2461.
- [8] Cho, S. H., Yokota, M., Ito, M., Kawasaki, S., Jeong, S. B., Kim, B. K., & Kaneko, K. (2014). Electrical disintegration and micro-focus X-ray CT observations of cement paste samples with dispersed mineral particles. *Minerals Engineering*, 57, 79-85.
- [9] Cho, S. H., Cheong, S. S., Yokota, M., & Kaneko, K. (2016). The dynamic fracture process in rocks under high-voltage pulse fragmentation. *Rock Mechanics and Rock Engineering*, 49, 3841-3853.
- [10] Blum, Hansjoachim. "Pulsed power Systems: Principles and applications." (2006).